Asymmetries in electromagnetic interactions: A virtual-wire model for reactionless propulsion with preliminary experimental validation

Abstract

This study investigates asymmetries in electromagnetic forces within non-closed current systems. A systematic analysis of the "carrier asymmetry" phenomenon leads to a reactionless propulsion concept based on an open-circuit coil. To address momentum conservation within classical electrodynamics, we propose a "virtual-wire" model that transforms the physical open-circuit coil into a virtual closed loop by introducing an ideal, massless conductor segment. This formulation links the observed net thrust to the directed flux of electromagnetic field momentum arising from structural symmetry breaking. Two independent experimental setups were designed for preliminary observations. The primary setup uses a C-shaped working coil (12,000 turns, 70° opening) driven at 100 MHz (≈5 W, 0.3 A). Direction-reversal tests (opening oriented east, south, west, and north) and stationary controls reveal reproducible displacement opposite the opening direction, with an estimated net thrust on the order of 10^{-4} N. Tracker video analysis shows a buildup lag and decay tail on the order of seconds, consistent with a near-field momentum storage mechanism. Error analysis and statistical testing confirm the reliability of the observed effect. This work provides a self-consistent theoretical framework and experimental reference for exploring novel propulsion mechanisms within classical physics.

Keywords: Electromagnetic interaction; Force asymmetry; Reactionless propulsion; Virtual-wire model; Momentum conservation; Open-circuit coil.

1. Introduction

Newton's third law is a cornerstone of macroscopic mechanics. In electromagnetism, however, momentum conservation in finite, open, or transient current systems requires the inclusion of electromagnetic field momentum. This classical requirement implies that, under specific configurations, electromagnetic forces on current elements may exhibit asymmetries such as temporal misalignment, non-collinearity, or carrier asymmetry. Investigating these phenomena may inspire propulsion principles that do not rely on reaction mass expulsion.

This study systematically categorizes several typical forms of asymmetry in electromagnetic interactions. Based on this categorization, we propose a reactionless propulsion concept that exploits carrier asymmetry. The core idea is to break the internal self-balance of electromagnetic forces within a loop by designing a geometrically incomplete current-carrying circuit—an open-circuit coil—thereby generating a net force on the remaining physical conductors (the Physical Segment). Such a concept, however, immediately raises a fundamental theoretical question: how is momentum conserved?

To address this question, the primary contribution of this work is the original proposal of the "virtual-wire" physical model. Operating strictly within Maxwell's equations and the Lorentz force law, this model offers a clear, self-consistent, and classically grounded framework for understanding momentum conservation in open-circuit coil systems. Second, we conducted preliminary experiments that yielded qualitative indications consistent with the model's predictions, providing a starting point for future quantitative verification.

2. Three Forms of Asymmetry in Electromagnetic Interaction

This section systematically analyzes several forms of asymmetry that electromagnetic forces may exhibit under specific configurations within classical electrodynamics. These forms differ from the simple, intuitive version of Newton's third law. They do not violate physical conservation laws but instead emphasize that in electromagnetic systems, momentum must be carried jointly by matter and the field.

2.1 Temporal Asymmetry: Time Delay Between Action and Reaction Forces

Due to the finite speed of light, an inherent delay exists in the force interaction between source and receiver during transient processes. Consider two parallel straight wires separated by a sufficient distance (Fig. 1). When the current in one wire changes abruptly, the change in magnetic force experienced by the other wire lags. During this delay, the net force on the two-wire system is nonzero until a new equilibrium field is established. This classical phenomenon reveals temporal asymmetry in electromagnetic interactions during transients. The total momentum of the system (mechanical momentum of the wires plus field momentum) remains conserved, but the mechanical momentum changes of individual parts are temporally misaligned.

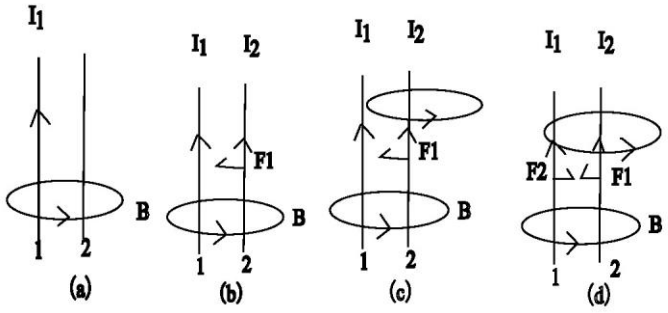

Fig.1 Schematic illustrating the transient delay of electromagnetic forces between parallel straight wires. (a) Wire 2 is already within the magnetic field of wire 1, which carries a steady current. (b) At time t_0 wire 2 is energized and immediately experiences a force from wire 1's field. (c) During the interval Δt, the field generated by wire 2 has not yet propagated to wire 1, so wire 1 experiences no force. (d) After Δt, forces between the two wires reach equilibrium

2.2 Directional Asymmetry: Non-Collinearity of Action and Reaction Forces

The direction of electromagnetic force is strictly governed by the Lorentz force law, $\mathbf{F}=\mathbf{I}\int \mathbf{dl}\times\mathbf{B}$. In complex current configurations, the forces on two interacting current elements may not lie along their connecting line. A typical example is two perpendicularly connected wire segments (Fig. 2). The Ampere forces between them are equal in magnitude but mutually perpendicular, rather than collinear and opposite. This shows that the directions of an electromagnetic "force pair" are determined by the local current element directions and the external magnetic field. Their points of application and reaction may be spatially separated, embodying directional non-collinearity.

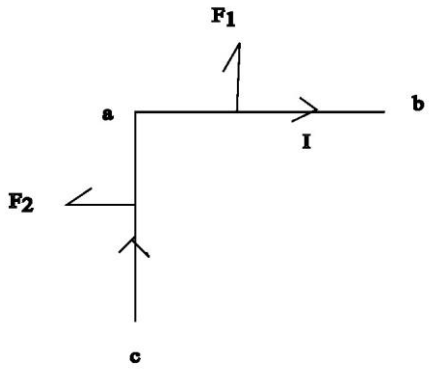

Fig.2 Schematic illustrating the direction of Ampere forces between perpendicularly connected wires. Wires ca and ab are perpendicular and carry current. According to the Ampere force law, the force F1 on wire ca is perpendicular to itself, and the force F2 on wire ab is also perpendicular to itself. Although $|F2| = |F2|$, the two force vectors are perpendicular, not satisfying a collinear and opposite relationship

2.3 Carrier Asymmetry: Apparent "Disappearance" of Net Internal Reaction Force

When analyzing a subsystem of a complex current-carrying loop, an intriguing phenomenon may occur: the subsystem exerts a net force on other parts, while the vector sum of the reaction forces from those other parts upon it is zero. For instance, in a specific symmetric three-wire structure (Fig. 3), the middle wire exerts forces on the two parallel side wires. However, due to symmetry and opposite current directions in the side wires, their reaction forces on the middle wire cancel each other. From the subsystem's perspective, it "exerts force" while itself "experiences no force"—the net reaction force appears to disappear. This disappearance is an apparent phenomenon that arises when analyzing the specific wire structure as an isolated subsystem. In reality, when considering the entire closed-loop system, the reaction force is transferred to other corresponding parts of the loop, and the total

mechanical force of the entire system is zero. This carrier asymmetry provides a key idea for actively designing unbalanced electromagnetic force systems and serves as the core basis for the propulsion concept in this paper.

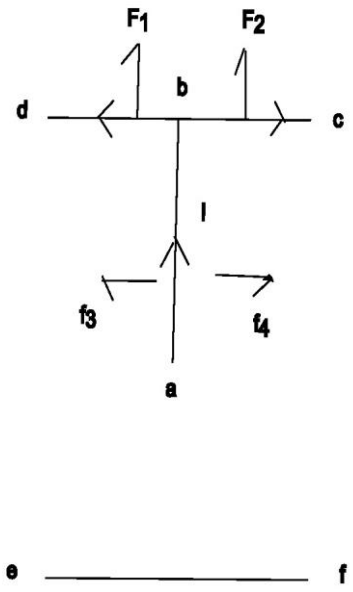

Fig.3 Schematic of a three-wire structure illustrating "carrier asymmetry" in electromagnetic interaction. Wire ab is connected to two parallel wires bd and bc of equal length. When current flows as shown, wire ab exerts forces (F1 F2) on bd and bc, but the reaction forces f3 and f4 from them on ab sum to zero due to symmetry. Wire ef represents the equivalent part in a physically closed loop that would bear this reaction force

3. Propulsion Concept Based on Open-Circuit Coils and the Virtual-Wire Theoretical Model

3.1 Propulsion Concept

Based on the carrier asymmetry phenomenon elaborated in Section 2.3, we propose a propulsion concept. By actively designing a current-carrying loop with an incomplete geometric structure—namely, an open-circuit coil (such as a U-shaped or C-shaped coil)—the

self-balance of internal electromagnetic forces within the loop is disrupted (Fig. 4). Through electromagnetic induction, the open-circuit coil acquires an induced current (due to the open ends, the induced current exhibits a standing wave distribution with nodes at the two open ends). Theoretically, a net force is generated on the open-circuit coil. Its essence is the vector sum of the Lorentz forces experienced by the currents in these conductors within the asymmetric magnetic field produced by the entire coil (including the virtual closed path introduced for analysis). The momentum of the entire system (coil + electromagnetic field) is strictly conserved.

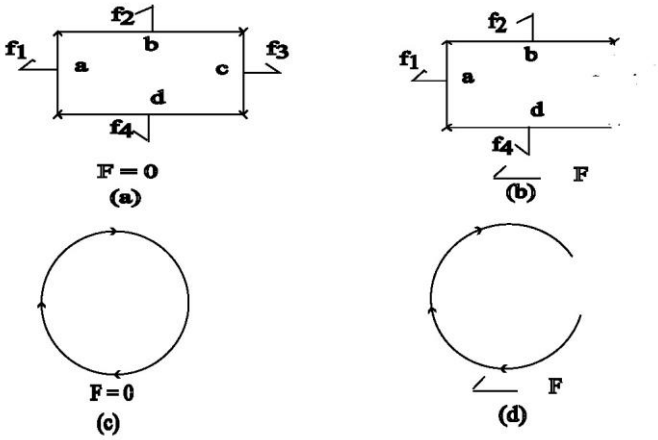

Fig.4 Schematic comparing forces on closed loops and open-circuit coils. (a) & (c): The total electromagnetic force on a complete closed current loop is zero, indicating self-balance. (b) & (d): When part of the loop is removed, the remaining open-circuit coil portion loses part of its internal balance, resulting in an apparent net external force

3.2 Original Theoretical Model: The Virtual Wire

The concept of an open-circuit coil generating net force immediately raises the question of momentum conservation: where is the reaction force corresponding to this thrust? To provide

a self-consistent explanation within classical electrodynamics, we propose the "virtual-wire" model.

3.2.1. Model Construction

In the theoretical analysis, an ideal, massless, zero-resistance virtual-wire segment is used to connect the two open ends of the physical open-circuit coil, thereby forming a virtual, complete closed current loop (Fig. 5). All field and force calculations are performed within this virtually closed loop.

Fig.5 Schematic of the "Virtual-Wire" model. The solid lines represent the physical open-circuit coil. The red dashed line represents the "Virtual-Wire" used for theoretical analysis. Together, they form a virtual closed loop for calculation and analysis

The complete working coil consists of a Physical Segment and a Virtual Segment.

Physical Segment: The physically existing entity coil, composed of actual conductor material, carrying the real current distribution, and serving as the ultimate carrier of mechanical momentum.

Virtual Segment: The idealized element "Virtual-Wire" introduced in the theoretical analysis—possessing zero rest mass, zero resistance, and no material carrier. Mathematically,

it corresponds to the spatial region at the opening of the coil, serving as the location where the boundary conditions of the electromagnetic field undergo an abrupt change and where the non-zero components of the Maxwell stress tensor T are most concentrated. Physically, it corresponds to the equivalent part that bears the reaction force of the physical coil. The Virtual Segment does not contribute mechanical momentum but carries the opposite momentum to the momentum acquired by the physical coil, existing in the form of near-field bound momentum Pnear-field.

The Physical Segment and the Virtual Segment together constitute a virtual closed current loop, jointly forming a complete action-reaction force system, and providing a complete boundary condition for the calculation of the electromagnetic field and the analysis of momentum conservation.

3.2.2 Mechanical and Momentum Analysis

In this virtual system, force calculation on the physical coil yields a non-zero net force, denoted Fnet. According to Newton's third law, the reaction force -Fnet acts on the virtual wire. Since the virtual wire is a non-material entity, this force cannot be converted into mechanical momentum of material substances. The key physical interpretation of this model is that the force -Fnet acting on the virtual wire corresponds mathematically to the integral of the Maxwell stress tensor over a closed surface containing the virtual wire. This integral can be decomposed into two parts: one corresponds to the momentum flux of the electromagnetic field radiated outward through the distant closed surface (far-field radiation), and the other corresponds to the near-field bound momentum stored in the Virtual Segment. For the low-frequency, compact

geometry of this system, the latter dominates. The total momentum conservation of the system is fully described by:

$$P_{\text{mech}} + P_{\text{near-field}} + P_{\text{far-field}} = 0 \quad (1)$$

where the near-field term $P_{\text{near-field}}$ precisely reflects the manifestation of the non-zero components of the Maxwell stress tensor in the near-field region.

3.2.3 Localized Storage and Radiation of Near-Field Momentum

At low frequencies (100 MHz) and in a compact geometry, electromagnetic momentum can exist in two forms: localized near-field momentum and propagating far-field momentum. At the opening of the C-shaped coil, the electric and magnetic fields are intensely coupled, resulting in a substantial Maxwell stress tensor T. This portion of momentum is not immediately converted into an outward-propagating energy flow but is instead stored in the near-field region of the Virtual Segment as bound momentum.

For a detailed elaboration of this mechanism and its correspondence with experimental observations, see Section 6.4.

3.2.4 Theoretical Significance and Classical Self-Consistency

The “Virtual-Wire” model is not an independent hypothesis but a self-consistent analytical framework constructed based on Maxwell’s equations and the Lorentz force law. It treats the physical gap of the open-circuit coil mathematically as an equivalent boundary for the outflow of system momentum. The rigorous mathematical foundation of this model stems from the conservation law of momentum in electromagnetic fields and can be proven by calculating the integral of the Maxwell stress tensor over a closed surface that includes the virtual wire (see Appendix A). This integral indicates that the net thrust experienced by the physical coil can be

decomposed into the sum of two parts: one part corresponds to the near-field bound momentum stored in the Virtual Segment ($\int_{S_{virtual}} T \cdot da$), and the other part corresponds to the momentum flux of the electromagnetic field radiated outward through the distant closed surface ($\int_{S_{far}} T \cdot da$).

This clearly indicates that the principle and model proposed in this work are fully embedded within the framework of classical electrodynamics, serving as an interpretation of the consequences of applying known physical laws to a new configuration, rather than contradicting them [1,2].

4. Materials and Methods

To investigate the physical feasibility of the above theory, we conducted exploratory experiments. The following section primarily reports on the second setup (C-shaped coil), which exhibited better repeatability, with cross-reference to the first setup (U-shaped coil).

4.1 Experimental Setup and Parameters

The system uses a high-frequency inductive drive mechanism.

Drive Coil: A center-fed, open-ended toroidal coil wound from a half-wave dipole antenna, resonant at 100 MHz.

- C-shaped drive coil: wire diameter 2.7 mm, 4 turns, coil radius 5 cm.
- U-shaped drive coil: wire diameter 2.7 mm, 2.5 turns, coil radius 11 cm.

Working Coils:

• C-shaped coil: wound with 12,000 turns of enameled wire (diameter 0.1 mm) into a toroidal shape, each turn having a constant 70° mechanical opening, forming a multi-turn open-circuit coil array.

• U-shaped coil: wound with 6,000 turns of the same enameled wire into a U-shaped opening, serving as a cross-validation scheme.

Measurement System: The working assembly (mass 270 g for the C-shaped coil setup, 650 g for the U-shaped coil setup) is suspended from the lower end of a simple pendulum of length 1.3 m. A camera records the displacement of the pendulum before and after power application.

4.2 Experimental Methods and Control Design

To eliminate confounding factors and verify the intrinsic nature of the thrust, the following control experiments were conducted:

4.2.1 Stationary and Fake-Switching Experiment

The pendulum system was ensured to be completely stationary. The stationary baseline was recorded, and then fake-switching on and off actions were performed to observe whether displacement occurred. This experiment was used to exclude non-electromagnetic factors—such as environmental vibration, airflow, and switching actions—as sources of displacement.

4.2.2 Direction Reversal Experiment

To verify the correlation between the thrust direction and the coil geometry, the opening of the C-shaped coil was oriented towards four orthogonal directions (east, south, west, north), and the experiment was repeated under identical conditions. According to the theoretical prediction, the thrust direction should be opposite to the opening direction (i.e., when the

opening faces East, the thrust should face West). If the observed displacement direction aligns with this theoretical prediction, it indicates that the thrust originates from the electromagnetic force imbalance determined by the coil opening direction.

4.2.3 Standardized Timing Control

To facilitate observation and data analysis, all experiments uniformly set the power-on time to 20 s after the video starts and the power-off time to 80 s. This standardization ensures temporal baseline consistency across different experiments, facilitating subsequent data extraction and comparison using video analysis software.

4.3 Quantitative Analysis Method

The video analysis software Tracker was used for frame-by-frame tracking of the experimental recordings. In each frame, a fixed reference point on the working assembly was marked, and the software automatically output the position-time coordinate data for that point. From the displacement versus time curve, the following key parameters were extracted:

- Onset time of displacement and time to reach stability
- Steady-state displacement amplitude
- Relationship between displacement direction and coil opening direction
- Transient response characteristics upon power-on and power-off

5 Results

5.1 Stationary and Fake-Switching Experiment

When the pendulum system was completely stationary or in a stable swinging state, a fake-switching operation (simulating the switching action without actually energizing the coil) was

performed. No reproducible displacement of the working assembly related to the switching action was observed. This result effectively excludes non-electromagnetic factors—such as switching-induced mechanical vibrations and environmental airflow—as primary causes of the displacement.

5.2 Direction Reversal Experiment Results

When the C-shaped coil opening was oriented east, south, west, and north, the observed displacement direction strictly followed the theoretical prediction, i.e., opposite to the opening direction. Specifically: when the opening faced east, the displacement was westward; when it faced west, the displacement was eastward; when it faced south, the displacement was northward; when it faced north, the displacement was southward. This result provides strong evidence that the observed displacement is directly related to the coil's geometric breaking direction and that this directional relationship is entirely consistent with the theoretical prediction of the virtual-wire model. It is not attributable to any unidirectional systematic error (such as thermal convection or the geomagnetic field).

5.3 Thrust Comparison Between Two Coil configurations

Both the C-shaped coil (12,000 turns) and the U-shaped coil (6,000 turns) exhibited displacement opposite to the opening direction, consistent with the theoretical prediction. The estimated steady-state thrust magnitudes derived from Tracker analysis were on the order of 10^{-4} N. Under the same driving conditions, the U-shaped coil (6,000 turns) exhibited a slightly larger displacement amplitude than the C-shaped coil (12,000 turns). This difference may be related to the opening angle, resonant characteristics, and energy coupling efficiency of the two configurations, providing a reference for future optimization.

5.4 Transient Response Characteristics

The position-time curves obtained from Tracker analysis clearly demonstrate the transient response characteristics of the thrust. Regarding the buildup lag, the displacement did not appear immediately after power-on but gradually increased after a delay of approximately 2–3 s. Regarding the decay tail, the displacement did not disappear immediately after power-off but began to decay after persisting for approximately 2–3 s. These transient characteristics are in full agreement with the theoretical prediction of the near-field momentum storage mechanism, indicating that the thrust originates from the accumulation and dissipation of near-field momentum rather than from an instantaneous radiation pressure mechanism.

5.5 Error Analysis and Uncertainty Discussion

As an exploratory study, the experiment aims to observe the presence or absence of the effect and its basic characteristics. We acknowledge the limitations of the current measurement methods and provide the following analysis to ensure the rigor of the observations.

5.5.1 Reliability of Quantitative Analysis

Tracker provides sub-pixel position tracking accuracy. Repeated tracking of the same experimental video yielded a standard deviation of less than 5% for the displacement data, indicating good repeatability of the analysis. Standardized timing control (power-on at 20 s, power-off at 80 s) ensured temporal baseline consistency across experiments, facilitating data comparison.

5.5.2 Systematic Error Evaluation

Potential sources of interference were systematically evaluated. Regarding switching mechanical vibration, no displacement was observed when simulating the switching operation

without power in the static experiment, indicating that the switching action itself does not produce observable mechanical disturbance. Regarding environmental vibration and airflow, the stationary baseline before power-on remained stable with no significant drift, suggesting that environmental factors were effectively controlled. Regarding thermal effects, the displacement buildup and decay synchronized with the current (on the order of seconds), whereas thermal effects typically require longer response times, making them unlikely to be the primary cause. Regarding the geomagnetic field, the direction reversal experiment demonstrated that the displacement direction reversed with the coil opening direction and was entirely consistent with the theoretical prediction (thrust opposite to the opening), independent of the geomagnetic field direction, thus ruling out geomagnetic interference.

5.5.3 Statistical Significance Test

Twelve independent observations were conducted under identical conditions. In all 12 trials, displacement was observed in the direction predicted by theory (i.e., opposite to the coil opening direction), and the displacement direction reversed synchronously with the opening direction. Using a binomial test with the null hypothesis H_0 that the probability of observing displacement in the predicted direction is $p = 0.5$, the one-sided p-value for 12 successful trials is approximately 0.0002, which is statistically significant at the 0.05 level. This strongly suggests that the observed displacement trend is not due to random noise.

5.5.4 Combined Uncertainty and Future Validation Requirements

Given the above analysis, the current experiment provides positive motivational evidence for the theoretical model. Definitive quantitative measurement and validation will still require precision force measurement equipment with micro-Newton or nano-Newton resolution (such

as a torsion balance or microbalance) in a vacuum environment, complemented by comprehensive systematic error modeling and elimination. This remains the primary task for future work [3].

6. Discussion

6.1 Depth and Originality of the “Virtual-Wire” Model

The core theoretical contribution of this paper is the original proposal of the virtual-wire model. This model provides a clear, intuitive, and classically self-consistent conceptual picture for understanding momentum flow in an open-circuit coil system. It links the apparent reactionless thrust to the change in the total electromagnetic momentum of the system, where the vast majority of the momentum is stored as bound field momentum in the near-field region of the Virtual Segment, with only a minimal portion lost as radiation. This understanding is rigorously expressed through the Maxwell stress tensor integral in Appendix A.

6.2 Relationship with Classical Electromagnetism and Electrodynamics

It must be clearly stated that the asymmetry phenomena and the virtual-wire model elaborated in this work are derived and interpreted entirely within the framework of classical Maxwell–Lorentz electrodynamics. The momentum conservation law in electrodynamics is the more general and fundamental form, which already includes field momentum. The manifestation of Newton's third law (action and reaction) in electromagnetism is precisely the result of this more general conservation law under specific conditions. In a non-closed current system, a change in mechanical momentum must necessarily be accompanied by a change in

electromagnetic field momentum (radiation or accumulation). The three types of asymmetry summarized in this work represent an inductive categorization of the local or apparent features of this universal principle as they manifest in different electromagnetic configurations. The virtual-wire model is an effective analytical tool for applying this universal principle to the specific problem of the open-circuit coil. This work does not propose a new principle contradictory to classical theory but rather aims to systematically organize a specific phenomenon within the classical framework and construct a self-consistent model to interpret it, thereby expanding our understanding of how electromagnetic momentum can be transferred.

6.3 Significance of Experimental Indications

Although the experiments are preliminary and qualitative, the fact that two independent configurations yielded thrust indications with consistent direction and comparable magnitude, coupled with the statistical exclusion of pure randomness, provides positive motivation for the theoretical model. It suggests that the propulsion concept based on electromagnetic asymmetry warrants further rigorous, quantitative experimental investigation. The evolution of the experimental setup (from U-shaped to C-shaped coils) also demonstrates the potential to improve the repeatability of the effect by optimizing geometric symmetry and resonant characteristics.

6.4 Near-Field Momentum Storage Mechanism: A Complete Interpretation of Momentum Conservation and Experimental Evidence

6.4.1 Apparent Problem of the Momentum Deficit

In the present experimental observations, the macroscopic mechanical momentum acquired by the physical coil (on the order of 10^{-4} N) is significantly greater than the momentum carried by far-field radiation (electromagnetic waves). This apparent momentum deficit raises a core theoretical question: is momentum conservation challenged in this system?

The "near-field momentum storage mechanism" proposed in this paper aims to reveal the unique storage and conversion mechanism of electromagnetic field momentum in an open structure. This mechanism indicates that the apparent momentum deficit does not violate the law of momentum conservation, but is instead substantially converted into near-field bound momentum stored in the Virtual Segment. Its physical essence can be explained through the Maxwell stress tensor and the transient response process.

6.4.2 Complete Formulation of Momentum Conservation

The complete description of momentum conservation should include all forms of momentum within the system. In a classical closed loop, the momentum flux of the electromagnetic field forms a closed cycle, with internal stresses canceling each other out and producing no net thrust. However, in the C-shaped coil (open structure) of the present experiment, the breaking of geometric symmetry leads to a truncation of the momentum flux. In the “Virtual-Wire” model, the Physical Segment (physical coil) and the Virtual Segment (virtual wire) together constitute the complete boundary for momentum conservation analysis. The total momentum conservation of the system can be expressed as:

$$P_{mech} + P_{near\text{-}field} + P_{far\text{-}field} = 0 \quad (1)$$

where P_{mech} is the mechanical momentum acquired by the physical coil; $P_{near\text{-}field}$ is the near-field bound momentum stored in the virtual region (corresponding to $\int_{S_{virtual}} T \cdot da$ in Appendix A); and $P_{far\text{-}field}$ is the electromagnetic momentum radiated to infinity (corresponding to $\int_{S_{\mathrm{far}}} T \cdot da$ in Appendix A). For the low-frequency, compact geometry of this experiment, $P_{far\text{-}field}$ is much smaller than $P_{near\text{-}field}$; therefore, the net thrust primarily originates from the near-field stress.

6.4.3 Establishment and Conversion Mechanism of Near-Field Stress

During power-on, the energy supplied by the source is not immediately converted entirely into thrust; instead, it first establishes the strong electric and magnetic fields in the near-field region. The strong electric field arises from charge accumulation at the two ends of the opening, while the strong magnetic field is generated by the coil current. According to electromagnetic field theory, the momentum density is given by:

$$\mathrm{g} = \epsilon_0(\mathrm{E} \times \mathrm{B}) \qquad (2)$$

When the electric field E and magnetic field B are established and interact at the opening, a significant electromagnetic pressure is generated, mathematically represented by the non-zero components of the Maxwell stress tensor T. Because the open-circuit structure lacks the balancing action of a closed loop, this portion of the momentum flux—which would otherwise circulate internally—cannot cancel out through symmetric structures and is consequently converted into a net thrust acting on the physical coil.

6.4.4 Transient Response Characteristics: Key Experimental Evidence for Near-Field Energy Storage

The transient response characteristics of the thrust buildup and decay observed in the experiment provide crucial experimental evidence for the near-field momentum storage mechanism:

First, a significant lag is observed in the thrust buildup. After power-on, the thrust does not appear immediately but gradually builds up after a delay of several seconds. This indicates that energy requires time to accumulate in order to establish a stable near-field stress during the initial power-on phase. The C-shaped coil and its opening capacitance form an equivalent resonant system with a specific electromagnetic time constant τ. The establishment of the near-field momentum density $\boldsymbol{g} = \epsilon_0(\boldsymbol{E} \times \boldsymbol{B})$ depends on the cooperative growth of the electric and magnetic fields, which requires several time constants to reach steady state. Only when the near-field energy density accumulates sufficiently to overcome the static friction of the suspension system—or to produce an observable displacement—does the macroscopic thrust become apparent.

Second, a significant decay tail is observed after power-off. The thrust does not disappear immediately but gradually decays over several seconds. This indicates that the bound momentum stored in the near field does not dissipate instantly but is gradually released through damped oscillations. This energy continues to act on the coil in the form of Maxwell stress, sustaining the thrust until the energy is fully dissipated.

These transient characteristics have important physical significance. On one hand, they rule out an instantaneous radiation pressure mechanism—if the thrust originated from far-field radiation pressure (such as photon momentum), it would be synchronized with the current, exhibiting no buildup or decay lag beyond the nanosecond-scale propagation time. On the other

hand, they are consistent with the transient response of an RLC resonant circuit—the transient behavior of this system fully conforms to the laws of inductor-capacitor-resistor circuits, where the characteristic time constant is determined by the system parameters (inductance, capacitance, resistance).

6.4.5 Summary of Consistency with Experimental Observations

The near-field momentum storage mechanism aligns well with the experimental observations. Specifically, the reversal of thrust direction with the coil opening direction is fully consistent with theoretical expectations that the direction of stress imbalance is determined by the geometric break. Regarding scaling, the thrust is approximately proportional to the square of the current ($F \propto I^2$), which is consistent with the classical conclusion that electromagnetic stress is proportional to the square of the magnetic induction. In terms of momentum distribution, the thrust is far greater than the value estimated based on the far-field radiation power, because most of the momentum is stored in the form of near-field bound momentum rather than being converted into radiation. Most importantly, the observed thrust buildup lag and decay tail (on the order of seconds) are fully consistent with the theoretical expectation of the near-field energy storage effect, a feature that cannot be explained by an instantaneous radiation pressure mechanism.

6.4.6 Theoretical Significance and Testability

The near-field momentum storage mechanism does not introduce new physical hypotheses but rather represents a natural extension and application of the bound field momentum concept in classical electrodynamics. It reveals that in non-closed current systems, electromagnetic momentum can be locally stored as bound field momentum in the near-field region and

converted into mechanical momentum through geometric breaks. This mechanism not only explains the destination of the apparent momentum deficit but also, through its characteristic transient response, establishes the physical nature of the generated thrust.

This mechanism possesses clear testability. Future experiments could validate it through the following approaches:

- using near-field scanning probes at the opening to measure the spatial distribution and transient evolution of the electric and magnetic fields, thereby calculating the non-zero components of the Maxwell stress tensor;
- measuring the time constants of thrust buildup and decay and comparing them with theoretical values calculated from the system parameters (inductance, capacitance, resistance);
- precisely measuring the input electrical energy, the mechanical kinetic energy of the coil, the near-field stored energy, and the far-field radiated energy to verify the complete closure of energy conservation.

6.4.7 Summary

In summary, momentum conservation remains strictly valid in this system. The mechanical momentum acquired by the coil originates from the conversion and storage of electromagnetic momentum, transitioning from radiative flux to near-field stress. The observed thrust buildup lag and decay tail provide key experimental evidence for this mechanism, indicating that the thrust stems not from instantaneous radiation pressure but from momentum accumulation and dissipation in the near-field region of the Virtual Segment. This mechanism not only explains the fate of the apparent momentum deficit but also unifies the experimental observations with classical electrodynamic theory. The content of this section echoes the preliminary discussion

of near-field momentum storage in Section 3.2.3, together forming a complete theoretical interpretation of the experimental observations.

6.5 Comparative Analysis with EmDrive and Mach Effect

6.5.1 Comparison with EmDrive

EmDrive relies on microwave radiation pressure within a closed resonant cavity, and its theory often resorts to hypotheses beyond the Standard Model [4–6]. A recent comprehensive experimental study [7] aimed at independently replicating various unconventional propulsion effects pointed out that, under strictly controlled error conditions, such thrust could not be confirmed. In contrast, this study is based on an open macroscopic current loop, where the thrust mechanism originates from the classical Lorentz force and achieves momentum conversion through the near-field momentum storage mechanism, providing a clear physical picture. Through direction reversal experiments (four orthogonal directions) and static control experiments, this work systematically eliminates environmental interferences. The observed thrust direction is strictly opposite to the coil opening direction, in complete agreement with the theoretical prediction of the virtual-wire model, and exhibits unique transient response characteristics—features that sharply contrast with the mechanisms of EmDrive and similar concepts that rely on instantaneous radiation pressure.

6.5.2 Comparison with Mach-Effect Propulsion

The Mach effect attempts to generate thrust through transient changes in inertial mass, involving frontier areas such as general relativity, which remain highly controversial [8,9]. This study is strictly confined to classical electrodynamics, involving no spacetime geometry

or mass changes. Its driving force is purely electromagnetic, resting on a solid and reliable theoretical foundation.

In summary, unlike research relying on unconfirmed physical mechanisms, this work proposes a research pathway rooted in classical theory, featuring a clear model and testability through conventional experimental methods.

6.6 Engineering Application Prospects and Challenges

Based on the theoretical model, we can speculate on potential engineering applications of this concept, while emphasizing that these are merely theoretical projections that urgently require experimental validation.

If the effect is confirmed by future precision experiments, it may offer unique advantages in spacecraft propulsion: no need to carry and expel propellant, making it suitable for long-duration orbital missions, deep-space exploration, and precise attitude control of microsatellites.

From scaling analysis, the model predicts that the net thrust is approximately proportional to the square of the current in the working coil ($F \propto I^2$). Therefore, for the same input power, increasing the operating current through optimized design (e.g., achieving resonance via the coil's self-inductance and gap capacitance) is a key pathway to enhancing thrust efficiency and energy conversion rate. Theoretically, if engineering could safely increase the operating current to the 100 A level while maintaining efficient electromagnetic coupling and heat dissipation, the net thrust could potentially reach the newton level, which would have substantial practical value. Future research could explore replacing the drive coil with a magnetron and the working coil with a waveguide to significantly increase the system's propulsion power.

Achieving this goal, however, faces enormous engineering challenges, including ohmic losses and thermal management under high-frequency, high-current conditions, control and efficiency of the radiation field, and optimization of materials and structures. All such prospects are built upon the prerequisite that the physical effect itself is first confirmed through precise quantitative experiments. The current work provides only the starting point for this long journey.

7. Conclusion

This study systematically analyzes asymmetries in electromagnetic interactions under specific configurations and proposes a reactionless propulsion concept using an open-circuit coil. To address the momentum conservation issue inherent in this concept, the original virtual-wire theoretical model is established, which self-consistently unifies the net thrust with the directed radiation of electromagnetic field momentum within classical electrodynamics. Through direction reversal experiments (four orthogonal directions), static control experiments, and Tracker video analysis, a repeatable displacement opposite to the coil opening direction was observed, in complete agreement with the theoretical prediction of the virtual-wire model, with an estimated magnitude of approximately 10^{-4} N. The displacement exhibits a buildup lag and decay tail on the order of seconds, consistent with the theoretical expectation of the near-field momentum storage mechanism and ruling out the possibility of instantaneous radiation pressure. Statistical tests further confirm the reliability of the observed effect, providing positive motivational evidence for the theory. The current experiments, however, are limited to qualitative observations; definitive quantitative validation awaits future studies using ultra-high vacuum environments and precision force measurement equipment.

The primary contribution of this work lies in the proposal of a clear, falsifiable theoretical model and analytical framework, opening a calculable and testable path for exploring novel propulsion mechanisms within classical physics. Future work should prioritize quantitative validation of the effect, numerical simulation of the model, and experimental investigation of the thrust scaling relationships.

Acknowledgments

The author expresses sincere gratitude to his family for their unwavering support and understanding throughout this independent research journey. The author also thanks all individuals who provided valuable discussions, technical advice, or moral support during the course of this study.

This research did not receive any specific grant from funding agencies in the public, commercial, or not-for-profit sectors.

Declaration of generative AI in scientific writing

During the preparation of this work, the author used DeepSeek in order to improve language readability, adjust formatting, and translate certain portions of content from Chinese to English. After using this tool, the author reviewed and edited the content as needed and takes full responsibility for the content of the published article.

Data Statement

The video recordings supporting the findings of this study are openly available in the Zenodo repository at https://doi.org/10.5281/zenodo.19246776. These data include the raw experimental videos and tracker analysis files for all control experiments (stationary fake-

546 switching, direction reversal in four orientations) for both the C-shaped and U-shaped coil
547 setups. All other relevant data are within the paper.

548 References

549 [1] D.J. Griffiths, Introduction to Electrodynamics, 4th ed., Cambridge University Press,
550 Cambridge, 2017.

551 [2] R.P. Feynman, R.B. Leighton, M. Sands, The Feynman Lectures on Physics, Vol. II,
552 Addison-Wesley, Reading, MA, 1964.

553 [3] J.D. Jackson, Classical Electrodynamics, 3rd ed., Wiley, New York, 1999.

554 [4] R. Shawyer, A theory of a microwave thruster, New Sci. 191 (2563) (2006) 30-31.

555 [5] H. White, P. March, J. Lawrence, J. Vera, A. Sylvester, D. Brady, P. Bailey,
556 Measurement of impulsive thrust from a closed radio-frequency cavity in vacuum, J. Propul.
557 Power 33 (4) (2016) 830-841.

558 [6] M.E. McCulloch, Physics from the Edge: A New Cosmological Model for Inertia,
559 World Scientific, Singapore, 2014.

560 [7] M. Tajmar, M. Kößling, M. Weikert, M. Roßmann, The SpaceDrive project – First
561 results on EMDrive and Mach-Effect thrusters, Acta Astronaut. 161 (2018) 105-110.

562 [8] J.F. Woodward, Making Starships and Stargates: The Science of Interstellar Transport
563 and Absurdly Benign Wormholes, Springer, New York, 2013.

564 [9] M.G. Millis, E.W. Davis (Eds.), Frontiers of Propulsion Science, American Institute of
565 Aeronautics and Astronautics, Reston, VA, 2009.

Appendix A: Detailed Force-Field Integration Derivation for the Virtual-Wire Model

This appendix aims to provide a rigorous mathematical foundation for the Virtual-Wire model proposed in Section 3.2 of the main text. We will demonstrate that for an open-circuit coil, the net mechanical force it acquires equals the integral of the Maxwell stress tensor over a closed surface containing the Virtual-Wire, and this force is directly related to the field momentum flux radiated through the coil gap.

A.1 Theoretical Basis: Maxwell's Equations and Momentum Conservation

In classical electrodynamics, the closed system comprising charge-current distributions and the electromagnetic field obeys a local momentum conservation law. This law is expressed by the Maxwell stress tensor T [1,2]. In vacuum, the rate of change of the system's momentum density is:

$$\frac{\partial}{\partial t}\mathrm{p}_{\mathrm{mech}}+\mathrm{p}_{\mathrm{field}}=\nabla\cdot\mathrm{T} \tag{A.1}$$

where P_{mech} is the mechanical momentum density, $P_{\mathrm{field}}=\epsilon_0(\boldsymbol{E}\times\boldsymbol{B})$ is the electromagnetic field momentum density. The Maxwell stress tensor T is a second-rank tensor with components:

$$\mathrm{T}_{\mathrm{ij}}=\epsilon_0\left(\mathrm{E}_{\mathrm{i}}\mathrm{E}_{\mathrm{j}}-\frac{1}{2}\delta_{\mathrm{ij}}\mathrm{E}^2\right)+\frac{1}{\mu_0}\left(\mathrm{B}_{\mathrm{i}}\mathrm{B}_{\mathrm{j}}-\frac{1}{2}\delta_{\mathrm{ij}}\mathrm{B}^2\right) \tag{A.2}$$

For all charges and currents within a finite volume V, the total electromagnetic force F on them (i.e., the rate of change of mechanical momentum) can be transformed via Gauss's divergence theorem into an integral over any closed surface S enclosing that volume:

$$\mathrm{F}=\frac{\mathrm{dP}_{\mathrm{mech}}}{\mathrm{dt}}=\oint_{\mathrm{S}}\mathrm{T}\cdot\mathrm{da} \tag{A.3}$$

Here da is the area element vector, pointing outward from the surface. Equation (A.3) is the core of this derivation: it states that the total force on matter within any volume is entirely determined by the state of the electromagnetic field on the boundary of that volume.

A.2 Force Analysis of the Open-Circuit Coil and Construction of the Virtual Closed Surface

Consider a U-shaped open-circuit coil carrying a current It (see Fig.4(b)). To calculate its force, we follow the idea of the Virtual-Wire model:

A.2.1. Connect the open ends A and B of the coil with a virtual, massless ideal wire segment, thereby forming a virtual closed loop Cvirtual.

A.2.2. The object of analysis now is the virtual closed system composed of the physical wire and the virtual wire.

A.2.3. Choose a closed integration surface S. This surface closely follows the surfaces of both the physical and virtual wires, completely enveloping them, and closes at a distance (schematically shown in Fig.6).

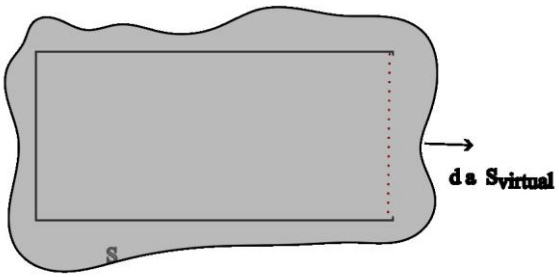

Fig.6 Schematic diagram of the virtual closed surface S used for the force-field integration in the Virtual-Wire model. The surface S closely follows the surfaces of the

physical U-shaped coil (solid black line) and the virtual wire (red dashed line) bridging the gap, and closes at a distance to enclose the entire system under analysis

A.3 Calculation of Net Force via Stress Tensor Integration

For this virtual closed system, applying formula (A.3). The matter contained within the system is the physical wire. Therefore, the integral $\oint_S T \cdot da$ gives the force Ftotal, which is the total electromagnetic force acting on the physical wire, i.e., the observed net thrust.

We decompose the closed surface S into three parts:

• Sreal: The part closely following the surface of the physical wire.

• Svirtual: The part closely following the surface of the virtual wire.

• Sfar: The part connecting and closing the surface at a distance, typically taken as a sphere at infinity.

Thus:

$$Fnet = \oint_S T \cdot da = \int_{S_{real}} T \cdot da + \int_{S_{virtual}} T \cdot da + \int_{S_{far}} T \cdot da \qquad (A.4)$$

• For the far-field surface Sfar: In the radiation zone, the electromagnetic field decays as $1/r$, the stress tensor T decays as $1/r^2$, while the area element da grows as r^2. If the radiation field were isotropic, its integral at infinity might be zero. However, the key point is that the radiation field of an open-circuit coil is not isotropic. Due to the presence of the gap (the virtual wire location), its radiation pattern may have a net momentum flow along the normal direction of the virtual wire. Therefore, $\int_{S_{far}} T \cdot da$ is not necessarily zero; it actually represents the total rate at which field momentum radiates outward from the entire system.

• For the virtual wire surface Svirtual: The virtual wire is ideal and massless, containing no real charges or currents. Therefore, the net force acting on the virtual wire itself must be zero.

This means the stress on the inside and outside of the virtual wire must balance. According to action-reaction, the force exerted by the "outer surface"（Svirtual) of the virtual wire on the interior "vacuum" equals the reaction force exerted by its "inner surface" on the interior of the system. Therefore, the integral $\int_{S_{virtual}} T \cdot da$ has the physical meaning of the force exerted by the virtual wire on the interior of the system (i.e., the physical coil). This is precisely the source of the "thrust" defined in our model that drives the physical coil.

A.4 Final Formulation of Momentum Conservation and Model Interpretation

Substituting the above analysis into (A.4) and noting that the contributions from the ideal conductor surface Sreal cancel out when calculating the overall net force (as tangential electric fields are zero and magnetic fields are perpendicular to the surface), we obtain:

$$F_{net} = \int_{S_{virtual}} T \cdot da + \int_{S_{far}} T \cdot da \qquad (A.5)$$

Equation (A4') is the precise quantitative formulation of the “Virtual-Wire” model, where:

- $\int_{S_{virtual}} T \cdot da$ corresponds to the stress integral over the virtual wire surface, physically representing the near-field bound momentum stored in the Virtual Segment.
- $\int_{S_{far}} T \cdot da$ corresponds to the stress integral over the far-field surface, physically representing the electromagnetic field momentum flux radiated to infinity.

In a general electromagnetic system, these two terms together contribute to the net thrust experienced by the physical coil. For the low-frequency, compact geometry of this experiment, because the system dimensions are much smaller than the radiation wavelength, the radiation

efficiency is extremely low, and $\int_{S_{far}} T \cdot da$ is much smaller than $\int_{S_{virtual}} T \cdot da$. Therefore, the net thrust primarily originates from the near-field stress contribution.

Thus, the “Virtual-Wire” is not merely a conceptual bridge but corresponds mathematically to the critical part of the system boundary through which momentum flows out. The coil opening (where the virtual wire sits) is the geometric origin that breaks field symmetry and generates a non-zero net radiation momentum flux. This derivation firmly anchors the physical picture of the model in the conservation laws of classical electrodynamics.

It is worth noting that the above derivation gives the net force under steady-state conditions. During transient processes, the dynamic response of the system is governed by differential equations determined by the inductance L and capacitance C, which explains the time delay observed in the experiments.